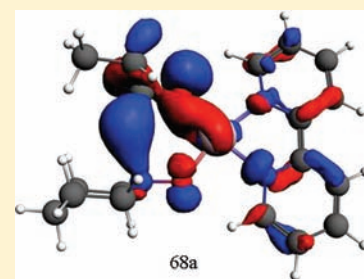


Cu(bipy)²⁺/TEMPO-Catalyzed Oxidation of Alcohols: Radical or Nonradical Mechanism?Paola Belanzoni,^{†,‡} Carine Michel,[§] and Evert Jan Baerends^{*,‡,||}[†]Department of Chemistry, University of Perugia, via Elce di Sotto 8, 06123 Perugia, Italy[‡]WCU program, Department of Chemistry, Pohang University of Science and Technology, San 31, Hyojadong, Namgu, Pohang 790-784, South-Korea[§]Université de Lyon, Institut de Chimie de Lyon, Laboratoire de Chimie, École Normale Supérieure de Lyon and CNRS, 15 parvis Descartes, 69 342 Lyon Cedex 07, France^{||}Chemistry Department, Faculty of Science, King Abdulaziz University, Jeddah, 21589, Saudi Arabia

Supporting Information

ABSTRACT: In the oxidation of alcohols with TEMPO as catalyst, the substrate has alternatively been postulated to be oxidized but uncoordinated TEMPO⁺ (Semmelhack) or Cu-coordinated TEMPO[•] radical (Sheldon). The reaction with the Cu(bipy)²⁺/TEMPO cocatalyst system has recently been claimed, on the basis of DFT calculations, to not be a radical reaction but to be best viewed as electrophilic attack on the alcohol C–H_α bond by coordinated TEMPO⁺. This mechanism combines elements of the Semmelhack mechanism (oxidation of TEMPO to TEMPO⁺) and the Sheldon proposal (“in the coordination sphere of Cu”). The recent proposal has been challenged on the basis of DFT calculations with a different functional, which were reported to lead to a radical mechanism. We carefully examine the results for the two functionals and conclude from both the calculated energetics and from an electronic structure analysis that the results of the two DFT functionals are consistent and that both lead to the proposed mechanism with TEMPO not acting as radical but as (coordinated) positive ion.



INTRODUCTION

A mild selective oxidation of primary alcohols to aldehyde has been developed by Gamez et al.¹ The original procedure is based on a bipy-copper complex and the 2,2,6,6-tetramethylpiperidinyl-1-oxyl (TEMPO) radical and a base (^tBuOK) as cocatalysts (see Figure 1).

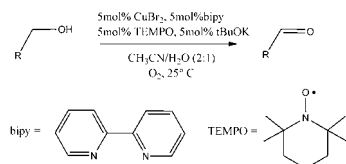
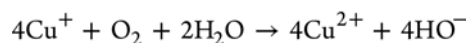
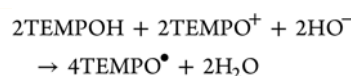
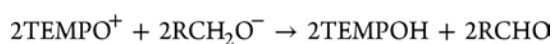
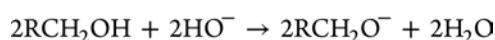
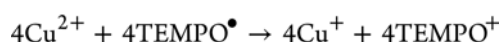
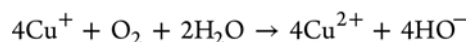
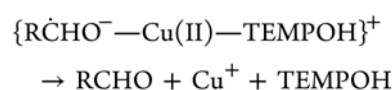
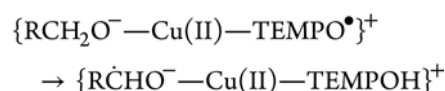
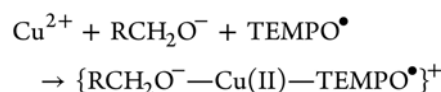
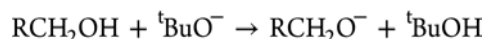


Figure 1. Catalytic oxidation of primary alcohols as proposed by Gamez et al.¹

The reaction mechanism is still under debate. Two main mechanisms have been proposed experimentally. The first one has been proposed by Semmelhack et al.^{2,3} A hydride (H[−]) is transferred from the alcoholate to the free TEMPO⁺ cation, as seen in the following mechanism (given here in a basic media):



In the second mechanism, proposed by Sheldon et al.,^{1,4} the alcoholate oxidation consists in a H[•] transfer to TEMPO[•]. This radical process is taking place in the copper coordination sphere



Received: April 7, 2011

Published: November 3, 2011

Recent experiments have provided experimental support for the nonradical nature of the reaction with coordinated TEMPO with Fe^{3+} instead of Cu^{2+} as the metal ion by MacMillan et al.⁵ In addition, the oxidation of the 4-nitrobenzylalcohol by a biphasic $\text{Cu(II)}/\text{TEMPO}$ catalyst has been followed by EPR by Fish et al.⁶ Despite the presence of Cu(II) and TEMPO^\bullet , this system is EPR silent during the reaction. This is an additional support for the nonradical nature of this mechanism, that is, for the Semmelhack mechanism. But the reaction is performed when Cu(II) and TEMPO are in the same phase, supporting a copper/TEMPO/alcohol complex, as in the Sheldon mechanism.

This mechanism is also debated in two recent theory papers, one by us⁷ and one by Wu et al.⁸ Both studies agree that the H_α -abstraction from alcoholate RCH_2O^- by the copper-coordinated TEMPO moiety represents the crucial step in the catalytic cycle for the alcohol oxidation into the aldehyde RCHO . But they have led to opposite results concerning the intrinsic nature of the reactive complex and the subsequent H-abstraction process being a hydride or a radical H-transfer.

In our paper, the theoretical investigation has shown that the Cu(bipy)^{2+} complex oxidizes the TEMPO radical to (coordinated) TEMPO^+ ion while Cu(II) is reduced to Cu(I) . The H-abstraction from alcohol by TEMPO^+ then proceeds as an intramolecular reaction (within the Cu coordination sphere), by transfer of H^- to the N of TEMPO, with a remarkably low calculated barrier (0.2 kcal/mol), see Figure 2, upper panel

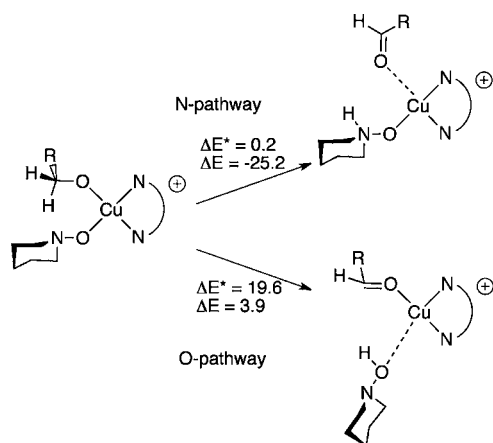


Figure 2. Two pathways have been proposed for the H-abstraction from the alcoholate by the TEMPO in the copper coordination sphere. The N-pathway has been studied at the OPBE level in our previous paper.⁷ The O-pathway has been studied by Wu et al.⁸ at the B3LYP level. The weak coordination of the aldehyde in the reaction intermediate in the N-pathway and of the TEMPOH in the reaction intermediate in the O-pathway are indicated with dotted lines.

(“N-pathway”). Thus, our proposal differs from both Semmelhack’s and Sheldon’s mechanistic proposals: it shares with Semmelhack the importance of oxidation of TEMPO^\bullet to TEMPO^+ to perform the H^- migration and it shares with Sheldon the feature that reaction takes place in the coordination sphere of Cu. A new element is that the reaction intermediate resulting from the H^- migration is an amine oxide, that subsequently will have to isomerize to the more stable $-\text{OH}$ product (hydroxylamine). Our study has been done using the OPBE functional. Wu et al.⁸ have revisited this mechanism using the B3LYP functional. According to those

calculations, H^\bullet abstraction from alcohol is performed by a copper-coordinated TEMPO^\bullet radical with Cu retaining its Cu(II) character, with a much higher reaction barrier of 19.6 kcal/mol. The H^\bullet is transferred to the oxygen of the TEMPO radical, see Figure 2 lower panel (“O-pathway”). This is the radical mechanism originally proposed by Sheldon,^{1,9,10} leading directly to the hydroxyl amine. In the calculations of ref 8, B3LYP puts the spin restricted closed shell singlet state 10.7 kcal/mol higher than the energy of a spin unrestricted electronic configuration. The latter was interpreted as having two antiferromagnetically coupled spins, one on TEMPO and one on Cu. This result is in disagreement with our DFT calculations with the OPBE functional, which gave the spin-restricted singlet state as the ground state for the starting $[\text{Cu(bipy)(alcoholate)(TEMPO)}]^+$ complex.¹¹

These conflicting results in the literature for the reaction mechanism pose a fundamental question about the reliability of the various exchange and correlation functionals in DFT methods: when different DFT calculations yield different results (B3LYP: radical/OPBE: nonradical mechanism), what should one believe?

It is important to try to obtain a mechanistic proposal independent of the DFT functional that is used. Our motivation to use the OPBE functional has been the reports in the literature that the B3LYP functional has severe problems in getting the relative energies of spin states in transition metal complexes right.^{12–14} Also for other properties (e.g., for geometries) the OPTX functional for exchange seems to perform reliably in transition metal complexes.^{15–17} Preferably, of course, the insight obtained from the functionals should be general, independent of the functional used. The electronic structure reason for a nonradical mechanism is not only based on the quantitative results of DFT calculations, it is also based on the insight obtained in earlier work on oxidation catalysis (see the analogy with ironoxo based oxidation catalysis emphasized in ref 7). The attack on the strong C–H bonds of alkanes and alcohols is performed by strongly electrophilic systems, using a low-lying acceptor orbital. Such an orbital is provided by the TEMPO π^* orbital, if it gets rid of the unpaired electron that occupies this orbital in the TEMPO radical, that is, when it becomes TEMPO^+ like. We will see that this electronic structure insight in the oxidation mechanism by oxoammonium ions holds regardless of the functional used.

In this article, we will reinvestigate the H-abstraction step using both OPBE and B3LYP functionals to determine the true nature of the reaction mechanism: radical (H^\bullet migration) or nonradical (H^- hydride migration). We will first investigate the key complex $[\text{Cu(bipy)(alcoholate)(TEMPO)}]^+$, in which the alcoholate and the TEMPO occupy adjacent coordination sites in the pseudo square planar coordination environment of Cu. Then, we will study the reaction barrier for both the OPBE and the B3LYP functional. We will show that the main difference between the two studies does not lie in the choice of different functional but in the choice of the pathway. Indeed, whatever the mechanism considered (radical or nonradical), the H-abstraction by TEMPO can follow two pathways: in the N-pathway, the H is abstracted by TEMPO nitrogen; in the O-pathway, the H is abstracted by the TEMPO oxygen (see Figure 2). In the absence of copper, the oxidation of alcohols in basic medium proceeds through the O-pathway, the oxidant being the oxoammonium cation.^{7,18} In our previous study,⁷ we have shown that the situation is reversed in the presence of copper: the reaction proceeds through a Cu-TEMPOH

intermediate, the H being bonded to the nitrogen and the copper to the oxygen (N-pathway). This intermediate is more stable than the reactant complex (by 25.2 kcal/mol) and the corresponding barrier is low (0.2 kcal/mol). The intermediate has the TEMPOH coordinated via a normal Cu-oxygen coordinative bond ($\text{Cu}-\text{O}(\text{TEMPOH}) = 1.87 \text{ \AA}$), but the formed aldehyde is much more loosely bound ($\text{Cu}-\text{O}(\text{aldehyde}) = 3.75 \text{ \AA}$). According to Wu et al.,⁸ the coordination to copper does not change the active site of TEMPO and the reaction follows an O-pathway. In the resulting Cu-TEMPOH, the TEMPO oxygen is only very weakly coordinated to the copper (4.87 Å). Now the aldehyde is strongly coordinated (1.87 Å). This intermediate is 3.9 kcal/mol higher in energy than the reactant complex and the energy barrier for this process is high (19.6 kcal/mol). Thus, one may wonder if the reaction path and the nature of the mechanism (radical or non radical) depends so strongly on the functional used.

COMPUTATIONAL DETAILS

DFT calculations on the systems (in gas phase) were performed using the ADF (Amsterdam Density Functional) package 2009.1,^{19–21} with a basis set of Slater type orbitals of TZP quality for all atoms. The inner core orbitals (up to 2p for Cu, 1s for C, N, and O) were treated by the frozen core approximation. Relativistic effects were included by using the zero-order regular approximation (ZORA).²² All calculations were performed both in the spin-restricted and spin-unrestricted approaches using both the B3LYP and the OPBE functionals. The latter is a combination of the OPTX²³ and the PBE functionals.²⁴ Convergence criteria for geometry optimization were 1×10^{-3} hartree in the total energy, 5×10^{-4} hartree/Å in the gradients, 1×10^{-2} Å in bond lengths, and 0.20° in bond and dihedral angles. TEMPO has been simplified by replacing the four methyl groups by hydrogen atoms, as in the calculations of Wu et al.⁸ and most of our calculations,⁷ and propanol has been chosen as substrate to be consistent with our previous work. The computational details are thus mainly the same as those reported in our previous paper,⁷ the only difference is that a smaller frozen core is presently employed for Cu (up to 2p instead of to 3p) in order to increase the accuracy in the 3d orbital energies.

THE INITIAL COMPLEX [Cu(BIPY)(ALCOHOLATE)(TEMPO)]⁺

We will first investigate the key complex $[\text{Cu}(\text{bipy})(\text{RO}^-)(\text{TEMPO})]^+$ (RO^- is the alcoholate), denoted **III** in our previous paper.⁷ Geometry optimization with the OPBE functional led to two conformers (**IIIa** and **IIIb**), which were almost isoenergetic (0.4 kcal/mol difference at the OPBE level). Those OPBE structures are rather similar to the two B3LYP conformers displayed in Figure 3 (OPBE-**IIIa** similar to the upper panel structure; OPBE-**IIIb** similar to the lower panel structure). Both complexes exhibit a pseudo square planar coordination environment of Cu (the angle between the CuNN and the CuOO planes is about 30°). The OPBE-**IIIb** has a short $\text{N}(\text{TEMPO}) \cdots \text{H}_\alpha(\text{RO}^-)$ distance. The short $\text{N}-\text{H}_\alpha$ distance reflects the bonding interaction between the occupied $\text{C}-\text{H}_\alpha$ donor orbital and the empty TEMPO^+ π^* like acceptor orbital. OPBE-**IIIa** has a long distance between the TEMPO N atom and the H_α of the alcoholate that is to be abstracted. Apparently the favorable interaction between $\text{C}-\text{H}_\alpha$ bond pair and empty TEMPO^+ π^* acceptor orbital is not operative in that conformation.

In this section we reinvestigate the ground state electronic structure of the $[\text{Cu}(\text{bipy})(\text{RO}^-)(\text{TEMPO})]^+$ complex with

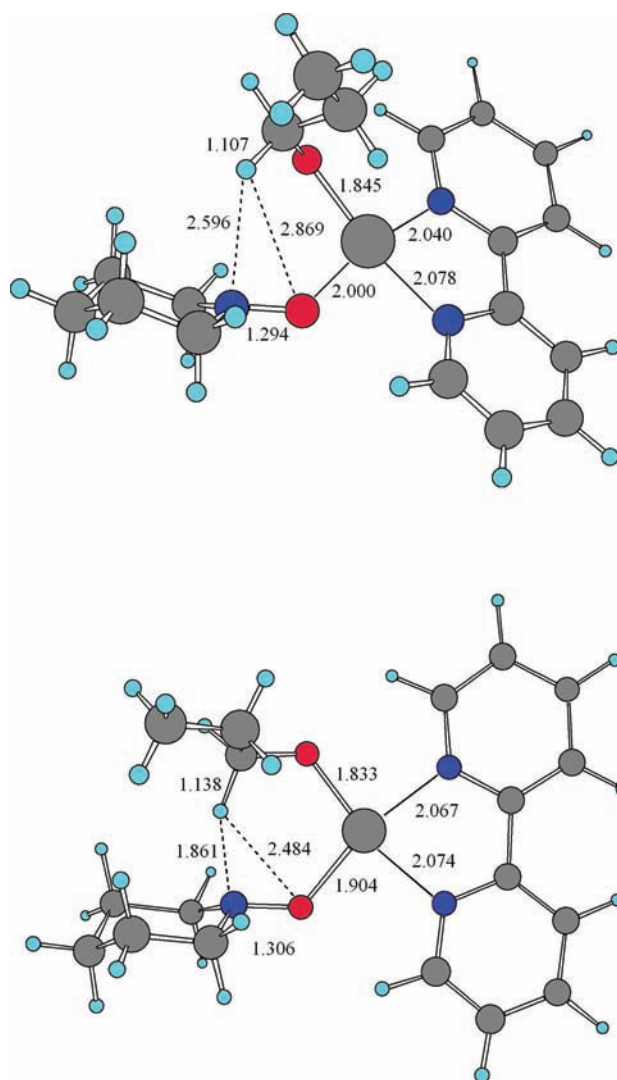


Figure 3. Optimized structure of complex **IIIunres** (upper panel) and of complex **IIIres** (lower panel) using the B3LYP functional.

the B3LYP functional and compare to the OPBE functional, in both spin restricted and unrestricted calculations.

Spin-Restricted Approach. Geometry optimization performed in the spin restricted approach using the B3LYP functional gave the structure shown in Figure 3 (lower panel, denoted as B3LYP-**IIIres**), where the Cu ion has square planar coordination, and TEMPO is coordinated to the Cu in an η^1 manner, only through the oxygen atom. The alcoholate hydrogen atom to be abstracted points to the nitrogen atom of TEMPO, at a distance of 1.861 Å, with a $\text{C}-\text{H}_\alpha$ bond 1.138 Å long. The **IIIres** structure is very similar to the **IIIb** structure obtained with OPBE.⁷

The molecular orbital (MO) level diagram of the B3LYP-**IIIres** complex is shown in Figure 4. It is similar to the one for the OPBE functional in Scheme 8 of ref.⁷ In particular the LUMO 72a has identically the same composition in the two cases, with 41% TEMPO- π^* character and 19% RO^- -HOMO, 17% Cu and 8% bipy character. The LUMO 72a is depicted in Figure 5. The main features of this orbital are as follows: (i) an antibonding interaction between the TEMPO π^* and the RO^- -HOMO; (ii) an antibonding Cu-bipy, Cu-TEMPO, and Cu-RO character. The antibonding interactions of the LUMO, largely delocalized over the five atoms of the coordination plane, have

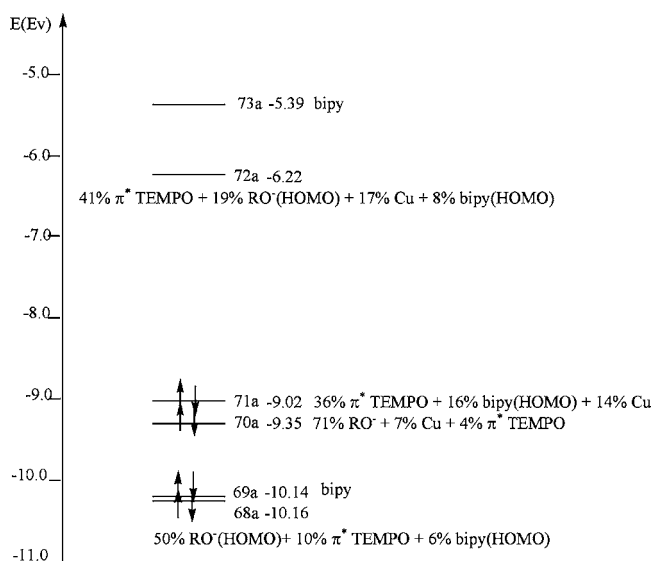


Figure 4. Molecular orbital level diagram of complex **IIIres** in the spin restricted closed shell singlet state at B3LYP level.

their bonding counterparts spread over a number of doubly occupied MOs, as for instance 71a and 68a, which are depicted also in Figure 5. In particular, 68a represents the bonding

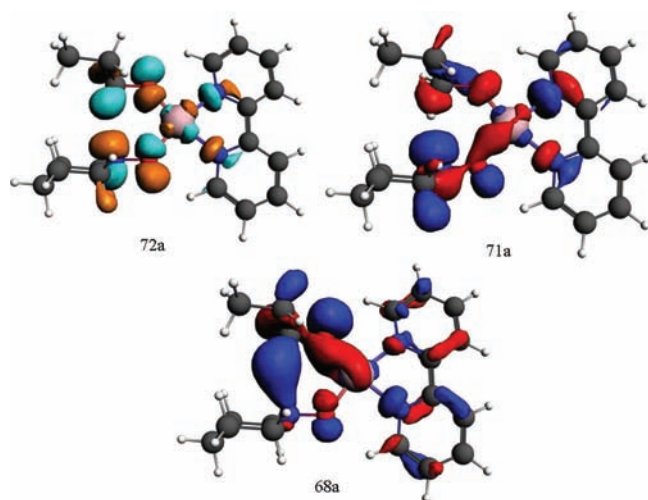


Figure 5. Relevant MOs of complex **IIIres** in the spin restricted closed shell singlet state at B3LYP level: LUMO 72a and HOMO 71a (top), and 68a MO (bottom).

interaction between the TEMPO π^* and the RO⁻ HOMO (and between Cu—RO), whereas 71a has bonding Cu $d_{x^2-y^2}$ -TEMPO π^* character. The similarity of the B3LYP orbitals with the corresponding orbitals obtained with the OPBE functional (see Figure 5 of ref 7) is striking.

From the Mulliken orbital populations for this complex B3LYP-**IIIres** reported in Table 1, the Cu 3d population (9.40) is close to 10, the TEMPO⁺ π^* LUMO acquires a substantial population of 1.10e and both the bipy HOMO and RO⁻ HOMO lose electron population (0.22e and 0.49e, respectively). These Mulliken orbital populations are virtually identical to those calculated at the OPBE level for the OPBE optimized **IIIres** conformer, see Table 1, as well as to those for **IIIb** in our previous paper (see Table 3 in ref 7). We note that

the electronic structure can be described as that of an initially empty π^* orbital of TEMPO⁺ which acquires considerable population (1.10 el.) by mixing, in a donor–acceptor interaction, into occupied orbitals of RO⁻ and Cu-bipy, thereby depleting those orbitals. The destabilized antibonding combination of the TEMPO⁺ π^* and RO⁻ and Cu-bipy orbitals is the LUMO 72a of the initial complex (the “reactant complex”) B3LYP-**IIIres**, see the composition of this orbital in Figure 4 and the plot in Figure 5. It should be clear that we do not imply that the charge on TEMPO is +1. The donation into π^* is so strong that in the end a population of \sim 1.10 el. in π^* results, not very different from the 1.0 el. in the π^* orbital in the free radical. The structural parameters, in particular the pyramidalization at N, can therefore be very much like those of neutral free TEMPO.

We conclude that the spin restricted singlet state calculations give closely similar results in terms of geometry, MO energy level diagram, and Mulliken orbital populations, whether using the OPBE or the B3LYP functional.

Spin Unrestricted Approach. We next turn to spin unrestricted calculations. In order to achieve different up and down spin orbitals, the SCF iterations have been started with a localized spin up electron on the metal and a spin down electron on the TEMPO ligand. As found by Wu et al.,⁸ geometry optimization using the spin unrestricted approach yields different results with the two functionals.

With OPBE, the calculation yields the same geometrical structure as in the spin restricted approach with the same bonding energy (OPBE-**IIIunres** = OPBE-**IIIres** = **IIIb**). An inspection of the electronic structure of OPBE-**IIIunres** shows two identical spin up and spin down orbitals, both equal to the closed shell orbitals obtained in the spin restricted calculation. The populations (Table 1) and the orbital shapes (similar to the restricted B3LYP ones in Figure 5) are identical to those of the restricted OPBE calculations.

With B3LYP, we found the geometric structure depicted in Figure 3 (upper panel) (denoted as B3LYP-**IIIunres**). The Cu has kept a distorted square planar (or distorted tetrahedral) coordination (the angle between the CuNN and the CuOO planes is 28.6°). More importantly, the alcoholate has bent away from TEMPO, so that the hydrogen atom to be abstracted is at a large distance from the nitrogen atom of TEMPO (2.596 Å) and even larger distance from the oxygen atom of TEMPO (2.869 Å). The C–H_α bond (1.107 Å) is little perturbed. This structure is actually reminiscent of the **IIIa** structure obtained (with spin restricted calculations) at almost equal energy to **IIIb** with OPBE in ref.⁷ The B3LYP-**IIIunres** structure is more stable than the optimized closed shell structure B3LYP-**IIIres** by 6.3 kcal/mol. Given the differences in, for example, basis set, this is in reasonable agreement with the finding by Wu et al.⁸ of 10.7 lower energy for the unrestricted calculation.

The electronic structure of B3LYP-**IIIunres** is truly different from the one of B3LYP-**IIIres** (and OPBE-**IIIb**). The MO diagram of B3LYP-**IIIunres** in Figure 6 shows that there is one unpaired β spin electron localized on an almost purely TEMPO π^* orbital (70a β) (indicated in red). The TEMPO π^*a orbital is unoccupied (cf. the almost purely π^* orbital 72a α). Although the total π^* population is 0.98 in B3LYP-**IIIunres** (see Table 1), which is close to the 1.10 of the restricted calculation, it has a very different origin: there is now an unpaired electron in the π^* , and there is virtually no electron donation out of the C–H bonding orbital into the TEMPO π^* .

Table 1. Fragment Analysis of Complexes IIIunres and IIIres (Initial), and IIITSunres and IIITSres (Transition State) Calculated Using the B3LYP and the OPBE Functional for the Two Pathways, the N-Pathway and the O-Pathway^a

Fragment	3d Cu ⁺	LUMO TEMPO ⁺	HOMO bipy	HOMO RO ⁻
B3LYP				
IIIres	9.40	1.10	1.78	1.51
IIIunres	4.91 α 4.40 β	0.05 α 0.93 β	0.96 α 0.84 β	0.91 α 0.74 β
Npath-IIITSres	9.52	1.20	1.84	1.27
Npath-IIITSunres	4.91 α 4.50 β	0.55 α 0.74 β	0.96 α 0.87 β	0.60 α 0.73 β
Npath-IIITSunreexcited	4.84 α 4.61 β	0.54 α 0.81 β	0.94 α 0.86 β	0.60 α 0.84 β
Opath-IIITSunres	4.82 α 4.71 β	0.64 α 0.69 β	0.92 α 0.90 β	0.57 α 0.61 β
OPBE				
IIIres (IIIunres)	9.39	1.10	1.79	1.48
Npath- IIITSres Npath- (IIITSunres)	4.75 α 4.75 β	0.62 α 0.62 β	0.92 α 0.92 β	0.61 α 0.61 β
Npath-IIITSunreexcited	4.87 α 4.49 β	0.55 α 0.85 β	0.95 α 0.77 β	0.57 α 0.83 β
Opath-IIITSunres	4.78 α 4.78 β	0.61 α 0.61 β	0.93 α 0.93 β	0.59 α 0.59 β

^aThe four fragments are the closed shell fragments Cu⁺, TEMPO⁺, bipy, and RO⁻. The gross populations of the relevant fragment molecular orbitals are given: the 3d population of the copper cation, the LUMO population of the TEMPO⁺, the HOMO population of bipy, and the HOMO population of the alcoholate RO⁻.

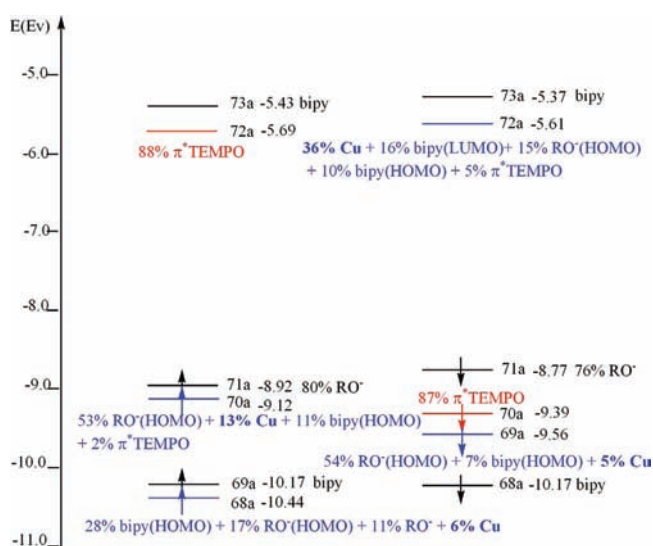


Figure 6. Molecular orbital level diagram of complex IIIunres in the spin unrestricted open shell singlet state at B3LYP level.

The three-electron repulsion of the unpaired π^* electron with the C–H bond pair causes the N \cdots H $_{\alpha}$ distance to become large. Concerning the distribution of the α spin density, it is not possible to clearly assign an unpaired α spin electron to Cu (or to any other single fragment). There is an excess α spin density on Cu (0.51 el.), but also on RO⁻ (0.17) and bipy (0.12). The Cu $d_{x^2-y^2}$ AO, which might be expected to contain the unpaired α electron,⁸ is actually involved in bonding interactions with all ligands (with the N lone pairs on bipy and the oxygen lone pairs on RO⁻ and TEMPO) in a series of lower lying orbitals. Indeed, non negligible Cu $d_{x^2-y^2}$ contributions can be found in 37a α (16%) (bonding with bipy) and 50a α (13%) (bonding with bipy and RO⁻), but small Cu $d_{x^2-y^2}$ contributions are also observed in 66a β (5%), 65a β (4%), and 56a β (6%). It is difficult to recognize two magnetic centers (which in this case should be the TEMPO radical and the Cu(II) ion) between which ferromagnetic or antiferromagnetic coupling can exist. Wu et al. report that they obtain a triplet which is higher in energy, and also find much higher transition energies for the

triplet.⁸ Hence we have not further explored triplet configurations.

In summary, we note that the differences between the functionals are not very large: The situation is that with OPBE the long N–H conformer (IIIa) is a tiny bit higher in energy (0.4 kcal/mol, see ref 7) than the short N–H conformer IIIb. With B3LYP it is just the other way around: unrestricted B3LYP has a minimum at the IIIa geometry, while restricted B3LYP has it at the IIIb geometry, 6.3 kcal/mol higher than the restricted B3LYP IIIa. On the unrestricted surface IIIb is a bit lower, i.e. only 2.5 kcal/mol above the unrestricted IIIa. We can say that both functionals have these two conformers practically degenerate, one (OPBE) tips the balance barely (0.4 kcal/mol) to IIIb, the other (unresB3LYP) just (2.5 kcal/mol) to IIIa.

It is remarkable that the B3LYP functional gives the lowest energy for a spin unrestricted electron configuration, while OPBE cannot lower the restricted energy by going unrestricted. However, the really important question is whether the reaction mechanism would be different according to the two functionals. We turn to this question in the next section.

■ TRANSITION STATE COMPLEX [CU(BIPY)(ALCOHOLATE)(TEMPO)]⁺ FOR THE H-ABSTRACTION STEP

Depending on the electronic structure of the reactant complex, one would expect a given mechanism:

- In IIIres (both OPBE and B3LYP), the C–H $_{\alpha}$ σ bond donates into the TEMPO⁺ π^* orbital, initializing a hydride migration.
- In B3LYP-IIIunres, the TEMPO holds a radical character, which could lead to a radical mechanism (H $^{\bullet}$ migration).

In addition to the nature of the H-abstraction (radical or nonradical), the reaction path is also an open question; it may depend on the functional choice. As we have seen before, the H can migrate to the nitrogen of TEMPO (N-pathway) or to the oxygen of TEMPO (O-pathway). We have shown that a H $^{\bullet}$ migrates from the alcoholate to the TEMPO nitrogen using the OPBE functional.⁷ Conversely, Wu et al. have claimed that a H $^{\bullet}$ migrates to the TEMPO oxygen, using the B3LYP functional.⁸

In this section, we study the reaction barrier for both the OPBE and the B3LYP functional for each pathway and analyze the radical character in each case. We have divided the discussion according to the reaction pathway.

N-Pathway. Energy and Geometry of the TS with B3LYP and OPBE Functionals. The energetics of the restricted and unrestricted paths are represented in Figure 7 for the two

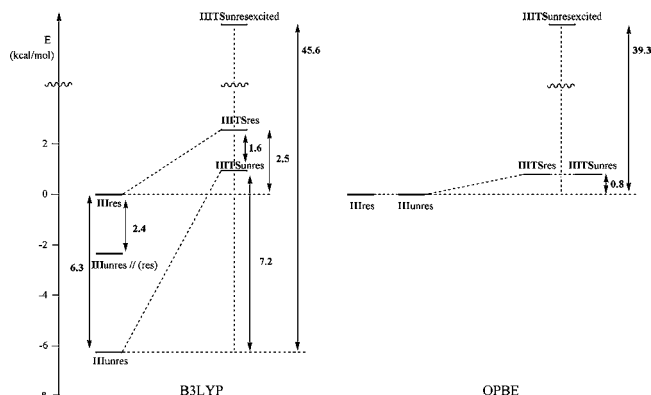


Figure 7. Energy profile for the H-abstraction step calculated in both the spin unrestricted open shell approach and in the spin restricted closed shell approach: B3LYP results (left) and OPBE results (right).

functionals: the B3LYP paths on the left-hand side, the OPBE paths on the right-hand side.

The spin restricted calculations give a “reactant complex” **IIIres** in which there is already dative bonding of the alcoholate C–H bonding electron pair to the empty TEMPO π^* with both functionals. This geometry will lead to a low transition barrier, since upon lengthening of the C–H bond, the corresponding bonding orbital will rise in energy and the favorable interaction will become much stronger.²⁵ Indeed, the energy of the OPBE-**IIITSres** and B3LYP-**IIITSres** remain low (0.8 and 2.5 kcal/mol respectively).²⁶ These barriers are in line with the OPBE results of ref.⁷ and considerably lower than the barrier of 19.6 kcal/mol reported by Wu et al.⁸

We turn now to the unrestricted calculations. Again, like for the “reactant complex”, the spin unrestricted OPBE calculations converge completely to the spin restricted solutions. We have verified that in the spin unrestricted OPBE-**IIITSunres** calculations we get two identical spin up and spin down orbitals, both equal to the closed shell orbitals obtained in the spin restricted OPBE-**IIITSres** calculations. To the right in Figure 7 the relative OPBE energies of the initial complex [Cu(bipy)(alcoholate)(TEMPO)]⁺ (**IIIres** = **IIIunres**) and the transition state complex (**IIITSres** = **IIITSunres**) for the H-abstraction step along the two (identical) spin unrestricted open shell and spin restricted closed shell singlet pathways are shown. The TS structure is, due to the larger basis sets we are using here, slightly different from the one in ref. 7: a N–H distance of 1.350 Å and a C–H_α distance of 1.335 Å.

Conversely, the B3LYP-**IIIunres** structure lacks the favorable dative interaction between the C–H bond and the TEMPO with its large distance between H_α and the TEMPO ligand. Thus, one may expect a higher barrier on the unrestricted path than on the restricted path. Working with the B3LYP functional, one could also start with putting the system in the electronically and geometrically favorable spin restricted configuration, with short H_α–N distance (see Figure 3, lower panel). This raises the energy by 6.3 kcal/mol, see Figure 7. We

have also checked if with the B3LYP-**IIIres** geometry of Figure 3, with the short H_α···N distance (1.861 Å), a single point spin unrestricted calculation would still yield a lower energy than the restricted one. That is the case, with unrestricted B3LYP calculations the short N–H structure **IIIb** is only 2.4 kcal/mol higher than the minimum at **IIIa** geometry. The difference between restricted and unrestricted B3LYP is energetically not so large. This is also the case for the transition state: the TS calculated by the unrestricted approach (denoted B3LYP-**IIITSunres**) is more stable than that calculated at the restricted approach (denoted B3LYP-**IIITSres**), but only by 1.6 kcal/mol. Thus, from the starting configuration to the TS, the differences between the unrestricted B3LYP path and restricted B3LYP path become smaller. In addition, the two corresponding transition state structures have the same geometry, which is depicted in Figure 8. The Cu ion has a square planar

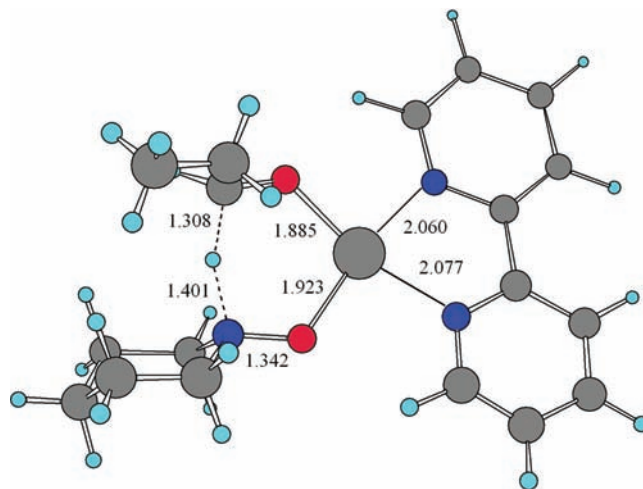


Figure 8. Transition state structure of **IIITSunres** (= structure of **IIITSres**) for the H-abstraction step from the B3LYP spin unrestricted open shell calculation ($\Delta E^\ddagger = 7.2$ kcal/mol).

coordination, with a N–H distance of 1.401 Å and a C–H_α distance of 1.308 Å. This is similar to the OPBE TS geometry. Finally, the most favorable B3LYP N-pathway is the unrestricted path: the H atom abstraction occurs with an activation energy of 7.2 kcal/mol. This barrier for the N-pathway is considerably lower than one reported by Wu et al.⁸ for the O-pathway (19.6 kcal/mol) and more in line with the OPBE results of ref. 7.

Electronic Structure of the N-Pathway Restricted TS. When analyzing the electronic structure of both the spin-restricted B3LYP and OPBE calculations, it becomes clear that they lead to precisely the same nonradical picture as the previous⁷ OPBE calculations: low barrier for H abstraction by N(TEMPO) due to increasing dative bonding of the C–H_α bonding orbital to the empty π^* upon C–H_α bond lengthening. The electronic structure of the TS is indeed very similar for OPBE-**IIITSres** and B3LYP-**IIITSres**. This is already apparent from the practically equal occupations of the fragments in the OPBE-**IIITSres** and B3LYP-**IIITSres** cases in Table 1. From Table 1 we see that the LUMO of TEMPO⁺ has acquired a substantial population (1.20 el. and 1.24 el. in B3LYP-**IIITSres** and OPBE-**IIITSres**, respectively), whereas the population of RO[−] has decreased from 2.0 el. to 1.27 el. and 1.22 el. for B3LYP-**IIITSres** and OPBE-**IIITSres**, respectively. We conclude that both the OPBE and B3LYP spin restricted

results for the populations and the orbital plots lead to the picture of strong dative bonding of the (stretched) C—H_α bond orbital to the TEMPO π* in the TS as the mechanism for strong lowering of the TS energy. This can be further substantiated by detailed consideration of the MO compositions. These results confirm the nonradical nature of the reaction mechanism.

Attempts at Electron Configurations with Radical Character in the N-Pathway Transition State. But should or could the *unrestricted* B3LYP calculations be interpreted in terms of a radical mechanism? A detailed analysis of both B3LYP-III TSres and B3LYP-III TSunres electronic structures does not allow such a conclusion. The molecular orbital (MO) level diagram for B3LYP-III TSunres is depicted in Figure 9.

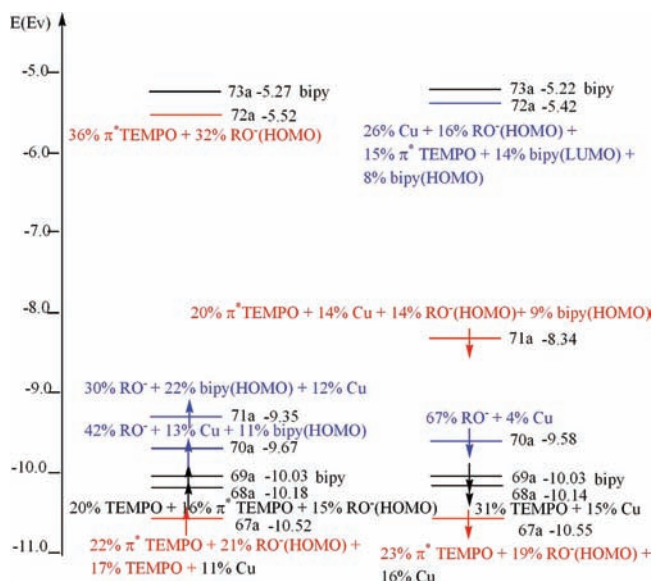


Figure 9. Molecular orbital level diagram of complex III TSunres in the spin unrestricted open shell singlet state at B3LYP level.

It is not easy to interpret this electronic structure. There is no longer a single MO that is predominantly of TEMPO π* character, and neither one of Cu- $d_{x^2-y^2}$ character. It is not so clear how precisely this electronic structure differs from the restricted one, since similar orbital interactions (bonding and antibonding) can be traced in the α and β spinorbital manifolds, although somewhat differently distributed over the orbitals. When we compare in Table 1 the populations for B3LYP-III TSunres with those of B3LYP-III TSres, we see that there are differences, but overall they are much less dissimilar than in the initial complexes B3LYP-III res and B3LYP-III unres. Quite strikingly the TEMPO π* α and β populations have become much closer (0.55 and 0.74 el., respectively), whereas they were widely disparate initially (0.05 and 0.93 el., respectively). We certainly can no longer speak of an unpaired electron in the TEMPO π*. In general the sum of the α and β populations in the B3LYP-III TSunres case is on each fragment close to the total population on that fragment in the restricted case B3LYP-III TSres. It appears that the B3LYP-III TSunres electronic structure has become rather close to that of B3LYP-III TSres, which is in line with the only 1.6 kcal/mol energy difference. There certainly is not a TEMPO radical present any more, and the explanation of the low TS barrier in terms of the donation out of the C—H bond orbital into the TEMPO π* is valid also with the B3LYP unrestricted theoretical model.

We have obviously not been able to generate with the spin unrestricted calculations two unpaired electrons that are antiferromagnetically coupled. During the SCF cycles strong rearrangements in many MOs occur and we can not force the initial unpaired β electron to remain localized on the TEMPO π* MO. The calculations converge to almost the spin restricted electronic structure. We have tried to generate a transition state which would contain the TEMPO radical in the H-abstraction step, by promoting the HOMO 71a β MO electron to the empty LUMO 72a β MO. So we have performed a single point spin unrestricted calculation, in the B3LYP-III TSunres geometry, by explicitly specifying the MO occupations for this excited state (71a β MO empty, 72a β MO occupied). It is denoted III TSunresexcited in Figure 7. The calculation converges to a non-Aufbau electronic structure where the π* character of the 72a β becomes more pronounced (now 25%, the largest contribution in 72a β). The π* character of the now empty 71a β MO reduces to 15%. One might feel that we have now approached more closely a situation with one unpaired β electron localized in the TEMPO π* (the largest contribution in the 72a β MO is 25% TEMPO π*, whereas the 72a α MO counterpart is empty) and one unpaired α electron in Cu $d_{x^2-y^2}$ (the 71a α MO has a remarkably large Cu $d_{x^2-y^2}$ percentage of 28%, whereas the 71a β MO counterpart is empty). It is still very far from a true radical picture with antiferromagnetically coupled unpaired electrons, and the energy is 45.6 kcal/mol above the initial III unres complex. Therefore, as shown in Figure 7, the energy barrier for a mechanism for the H-abstraction step in which the TS radical character is to some extent maintained on the TEMPO would be much higher than the nonradical one (7.2 kcal/mol).

We have tried to generate in the same way a TS state for a radical mechanism in the H-abstraction step with the OPBE functional, by promoting in the OPBE III TSunres case the HOMO 71a β MO electron to the empty LUMO 72a β MO, which has more TEMPO π* character. The calculation converges to a non-Aufbau electronic structure with an energy of 39.3 kcal/mol above the initial III unres complex. Therefore, as shown in the panel to the right of Figure 7, the energy barrier for a radical mechanism in the H-abstraction step would, with OPBE, be 39.3 kcal/mol, much higher than the nonradical one (0.8 kcal/mol). We conclude that both functionals, B3LYP and OPBE, provide a nonradical mechanism for the N-pathway of the H-abstraction step in the Cu(bipy)/TEMPO catalyzed oxidation of alcohols.

O-Pathway. Finally, we have considered the O-pathway that has been identified by Wu et al.⁸ as the reaction path: in the TS they have determined, the H migrates to the TEMPO oxygen that is also coordinated to Cu, see Figure 1 of ref 8. In the present section, we reconsider this pathway, at the B3LYP level and also at the OPBE level.

At the unrestricted B3LYP level, we have found the TS structure depicted in Figure 10, with an O—H distance of 1.295 Å and a C—H distance of 1.341 Å. The energy barrier is 19.7 kcal, identical (within the computational differences in basis set etc.) to the 19.6 kcal/mol found by Wu et al.⁸ This is much higher than the barrier for H abstraction by N, also with the B3LYP functional (7.2 kcal/mol). This high barrier does not depend on the functional used. At the OPBE level, the H migration to the oxygen of TEMPO encounters a barrier of 12.2 kcal/mol, and the corresponding transition state structure is similar to the B3LYP one with a O—H distance of 1.223 Å and a C—H distance of 1.358 Å. Once again using OPBE the

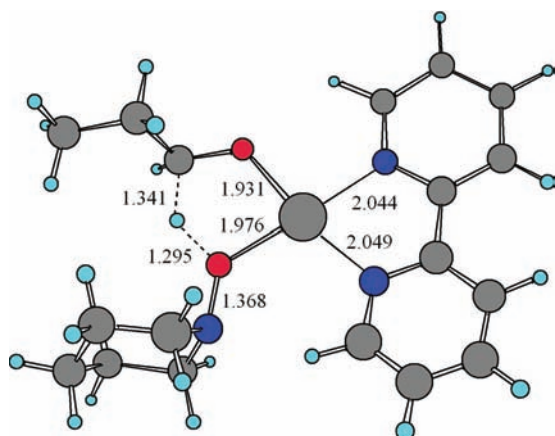


Figure 10. Transition state structure for H-abstraction by the TEMPO oxygen with B3LYP spin unrestricted calculations ($\Delta E^\ddagger = 19.7$ kcal/mol).

restricted and unrestricted calculations give the same result. Therefore, both OPBE and B3LYP indicate the N-pathway as preferred over the O-pathway, and the pathway does not depend on the functional. The O-pathway TS possibly requires more strain in the ligand framework, which would explain the higher energy. But this may lie also in the difference in the stability of the obtained products. After the H-migration to the oxygen of TEMPO, the resulting aldehyde is still coordinated to the copper while the protonated TEMPO is almost free, its oxygen being already bonded to the extra H. This situation is the reverse of the one for the N-pathway product. There, the aldehyde is almost free while the TEMPO protonated on the nitrogen is coordinated to the copper through its oxygen, fully available. At OPBE level the O-pathway product is 10.2 kcal/mol higher in energy than the N-pathway product. This may explain why the H-abstraction barrier is higher in the O-pathway than in the N-pathway.

Remains the question of the radical or nonradical nature of this O-pathway. Wu et al.⁸ claim this path to be a radical path based on the unpaired electron on TEMPO in the reactant complex B3LYP-IIIunres (IIIa conformation). Let us examine the transition state population analysis (see Table 1). At the OPBE level, it is striking that the population on the relevant fragment orbitals is almost the same in the two transition states (N-path-IIIITS and O-path-IIIITS). The population analysis therefore gives little evidence for a radical mechanism. One might argue that in the TS the bond is already formed to such an extent that the α and β spin orbitals making up the bond have already become equal. The only indication that there could be radical character is the dihedral angle between the O(TEMPO)–Cu–O(alcoholate) and N(bipy)–Cu–N'(bipy) planes. This is expected to be 90° (tetrahedral) for a Cu d^{10} electron configuration and 0° (square planar) for d^9 . In the IIIb type structures (both OPBE and B3LYPunres) as well as the N-pathway TS the angle is always ca. 30°, in rough agreement with our electronic configurations between d^9 and d^{10} . Only in the O-pathway TS the angle is 0°, as for a d^9 configuration. This is however very superficial evidence for a radical mechanism. Since electron shifts between metal and ligands (both TEMPO and alcoholate) can be achieved very simply by just changing orbital compositions, it is very difficult to track electron flow. Since the O-pathway is not followed anyway, we refrain from an in-depth study of the radical or nonradical nature of this hypothetical pathway.

CONCLUSIONS

We conclude from this investigation that the results of ref 7, which have been questioned in ref 8, do not depend on the use of the OPBE functional, but hold for the B3LYP functional as well. In short, the reaction mechanism for the aerobic oxidation of alcohols by the Cu(bipy)²⁺ and TEMPO• radical cocatalyst system appears to involve oxidation of the TEMPO• radical to TEMPO⁺ upon coordination of TEMPO to the Cu ion. This generates on the *coordinated* TEMPO an empty π^* orbital which can act as electrophilic acceptor orbital for the dative bonding by the C–H _{α} bonding electron pair. This interaction, and the H migration, take place in the coordination sphere of Cu (intramolecular). This reaction mechanism synthesizes elements of the Semmelhack^{2,3} mechanism, which emphasized the action of TEMPO⁺ as reactive intermediate, but did not view complexation to Cu as a necessary step, and the Sheldon^{9,27} mechanism, which emphasized that the reaction should be “Cu-centered”, but retained the TEMPO radical as reactive intermediate. The H is transferred as hydride, to the N of TEMPO. Transfer of H to the O of TEMPO is found to meet with a much higher barrier, regardless of the functional used. This pathway may be described as H• radical transfer, although it is not easy to substantiate this picture with population analyses. The first experimental investigations⁵ suggest that the complexation of TEMPO• radical to a transition metal ion with the generation of an electrophilic TEMPO⁺ ligand as reactive species may be more general than with just the Cu(bipy)²⁺ metal fragment. A recent investigation of TEMPO complexes of Ni²⁸ shows an interesting X-ray structure with a Ni-coordinated TEMPOH moiety with H bonded to the N of TEMPO.

We have found that the ground state of the initial [Cu(bipy)-(alcoholate)(TEMPO)]⁺ complex for the H-abstraction step does depend sensitively on the functional used: OPBE favors a spin restricted closed shell singlet state, whereas B3LYP favors a spin unrestricted electronic structure. However, we have also shown that upon further detailed analysis, comparing the transition state geometries and electronic structures in the H abstraction step of the catalytic cycle, the OPBE and B3LYP results give basically the same picture. We should caution that present day functionals are not quantitatively reliable. One should always invoke electronic structure analysis to make sure that intelligible results have been obtained. We have computed the energy difference for unrestricted minus restricted total energy for a series of 36 functionals, using always the same restricted B3LYP and unrestricted B3LYP geometries (IIIb and IIIa respectively). The restrictedIIIb-unrestrictedIIIa energy differences in Table 1 of SI vary over a wide range, with outliers from –30.7 kcal/mol (BHandHLYP) to +19.3 (LDA): black box use of present day functionals is not yet possible.

ASSOCIATED CONTENT

Supporting Information

A table with energy differences between unrestricted and restricted calculations at fixed geometries for 36 functionals, with discussion. This material is available free of charge via the Internet at <http://pubs.acs.org>.

AUTHOR INFORMATION

Corresponding Author

*E-mail: e.j.baerends@vu.nl.

ACKNOWLEDGMENTS

This research was supported by the National Research School combination "Catalysis by Design" (C.M., E.J.B.) and by the WCU (World Class University) program (P.B., E.J.B.) through the Korea Science and Engineering Foundation funded by the Ministry of Education, Science and Technology (Project No. R32-2008-000-10180-0).

REFERENCES

- (1) Gamez, P.; Arends, I. W. C. E.; Reedijk, J.; Sheldon, R. A. *Chem. Commun.* **2003**, 2414.
- (2) Semmelhack, M. F.; Schmid, C. R.; Cortés, D. A.; Chou, C. S. *J. Am. Chem. Soc.* **1984**, *106*, 3374.
- (3) Semmelhack, M. F.; Schmid, C. R.; Cortés, D. A. *Tetrahedron Lett.* **1986**, *27*, 1119.
- (4) Dijkman, A.; Arends, I. W. C. E.; Sheldon, R. A. *Org. Biomol. Chem.* **2003**, *1*, 3232.
- (5) Van Humbeck, J. F.; Simonovich, S. P.; Knowles, R. R.; MacMillan, D. W. C. *J. Am. Chem. Soc.* **2010**, *132*, 10012.
- (6) Contel, M.; Izuel, C.; Laguna, M.; Villuendas, P. R.; Alonso, P. J.; Fish, R. H. *Chem.—Eur. J.* **2003**, *9*, 4168.
- (7) Michel, C.; Belanzoni, P.; Gamez, P.; Reedijk, J.; Baerends, E. J. *Inorg. Chem.* **2009**, *48*, 11909.
- (8) Cheng, L.; Wang, J.; Wang, M.; Wu, Z. *Inorg. Chem.* **2010**, *49*, 9392.
- (9) Sheldon, R.; Kochi, J. *Metal-Catalysed Oxidations of Organic Compounds*; Academic Press: New York, 1981.
- (10) Gamez, P.; Arends, I. W. C. E.; Sheldon, R. A.; Reedijk, J. *Adv. Synth. Catal.* **2004**, *346*, 805.
- (11) Attempts to obtain with the OPBE functional a lower energy spin unrestricted configuration, with e.g. an α electron on Cu and a β electron on TEMPO, failed. The α and β spin orbitals after convergence proved to be equal, and the closed shell singlet state was recovered.
- (12) Swart, M.; Groenhof, A. R.; Ehlers, A. W.; Lammertsma, K. *J. Phys. Chem. A* **2004**, *108*, 5479.
- (13) Swart, M. *J. Chem. Theory Comput.* **2008**, *3*, 2057.
- (14) Güell, M.; Solà, M.; Swart, M. *Polyhedron* **2010**, *29*, 84.
- (15) Swart, M.; Ehlers, A.; Lammertsma, K. *Mol. Phys.* **2004**, *102*, 2467.
- (16) Conradie, J.; Ghosh, A. *J. Chem. Theory Comput.* **2007**, *3*, 689.
- (17) Schultz, N. E.; Zhao, Y.; Truhlar, D. G. *J. Phys. Chem. A* **2005**, *109*, 11127.
- (18) Bailey, W. F.; Bobbitt, J. M.; Wiberg, K. B. *J. Org. Chem.* **2007**, *72*, 4504.
- (19) SCM, *ADF2009.1, Theoretical Chemistry*; Vrije Universiteit: Amsterdam, The Netherlands, 2009; <http://www.scm.com/>.
- (20) Baerends, E. J.; Ellis, D. E.; Ros, P. *Chem. Phys.* **1973**, *2*, 41.
- (21) Fonseca Guerra, C.; Snijders, J. G.; te Velde, G.; Baerends, E. J. *Theor. Chem. Acc.* **1998**, *99*, 391.
- (22) van Lenthe, E.; Baerends, E. J.; Snijders, J. G. *J. Chem. Phys.* **1994**, *101*, 9783.
- (23) Cohen, A. J.; Handy, N. C. *Mol. Phys.* **2001**, *99*, 607–615.
- (24) Perdew, J. P.; Burke, K.; Ernzerhof, M. *Phys. Rev. Lett.* **1996**, *77*, 3865.
- (25) Louwse, M. J.; Baerends, E. J. *Phys. Chem. Chem. Phys.* **2007**, *9*, 156.
- (26) The OPBE-IIITS energy barrier is slightly higher than that we found in ref.⁷ which was 0.2 kcal/mol, because of the larger basis set and smaller frozen core we are now using for copper.
- (27) Gamez, P.; Aibel, P. G.; Driessen, W. L.; Reedijk, J. *Chem. Soc. Rev.* **2001**, *30*, 376.
- (28) Isrow, D.; Captain, B. *Inorg. Chem.* **2011**, *50*, 5864.